

# Quantitative Functionalization of the Tyrosine Residues in Silk Fibroin through an Amino-Tyrosine Intermediate

Kian G. Hausken, Romane L. Frevol, Kimberly P. Dowdle, Aleena N. Young, Jeremy M. Talusig, Carolynne C. Holbrook, Benjamin K. Rubin, and Amanda R. Murphy\*

Here, a reaction sequence that can be used to quantitatively modify the tyrosine residues in silk protein from *B. mori* silkworms is demonstrated. A primary amine is installed ortho to the hydroxyl group on the tyrosine ring using a diazonium coupling reaction followed by reduction of the azo bond. The resulting amine is then acylated using carboxylic acid or NHS-ester derivatives at room temperature and neutral pH conditions. The silk derivatives are characterized using  $^1\text{H}$  NMR, UV-vis spectroscopy, ATR-FTIR, and a unique method to follow this reaction sequence using isotopically labeled reagents and 2D NMR spectroscopy is also used. This study further demonstrates that this sequence can be used to install alkyne or azide functional groups which can undergo further bio-orthogonal cycloaddition reactions under mild conditions. Finally, methods to carry out these modifications on solid silk microparticles and electrospun mats are also described.

and aspartic/glutamic acid (1.1 mol%), so these are the sites typically targeted for chemical modification to customize the protein for a desired application.<sup>[9]</sup> While serine residues are most abundant, the poor reactivity of alcohol groups in aqueous media require the use of organic or ionic liquid solvents,<sup>[10–12]</sup> highly basic<sup>[13]</sup> or strongly oxidizing conditions.<sup>[14]</sup> Carbodiimide-mediated reactions targeting the carboxylic acid residues have been more widely used as they can be carried out in mild, aqueous conditions.<sup>[10,11,15–21]</sup> While simple to execute, silk has a very low number of carboxylic acids (1.1 mol%) which severely limits the density of functionalization possible with carbodiimide coupling. In addition, many biomolecules targeted for attachment to silk contain multiple

carboxylic acid or amine groups so exposure to carbodiimide reagents can result in crosslinking and inactivation.<sup>[22]</sup>

Silk contains an unusually high level of tyrosine ( $\approx 5.3$  mol%, 277 per protein),<sup>[8]</sup> so this amino acid has been a major target for modification. A few examples of cyanuric chloride-activated coupling,<sup>[19,23–25]</sup> as well as enzyme-catalyzed oxidation,<sup>[26]</sup> crosslinking,<sup>[27]</sup> and grafting<sup>[28,29]</sup> to tyrosine have been reported. However, the most highly used tyrosine modification with silk to date has been diazonium coupling.<sup>[10,22,30–42]</sup> While this reaction has found broad utility, it is not without limitations. While there are several commercially available aniline derivatives that can be attached to silk using a diazonium coupling reaction, it is not always straightforward to attach anilines to more complicated molecules for direct conjugation. Also, generation of the diazonium salt from the aniline derivative occurs under highly acidic conditions, which is not amenable to molecules containing sensitive functional groups. Most commercially available anilines containing alkyl amines are electron rich and have poor reactivity in diazonium coupling reactions<sup>[30,37]</sup> and cross-reactivity of amines with sodium nitrite is a concern. Therefore, the diazonium reaction has primarily been used to add simple anilines with acidic functional groups that modify the charge of the silk protein<sup>[31,32,34–36,39]</sup> or allow for subsequent functionalization.<sup>[10,22,33]</sup> A final drawback is that the reaction produces an azo chromophore that turns the silk dark orange-red, which makes imaging through films difficult and has been found to interfere with several optical bioassays.

Here, we developed an alternative strategy to functionalize the tyrosine residues in silk that builds on the success of diazonium

## 1. Introduction

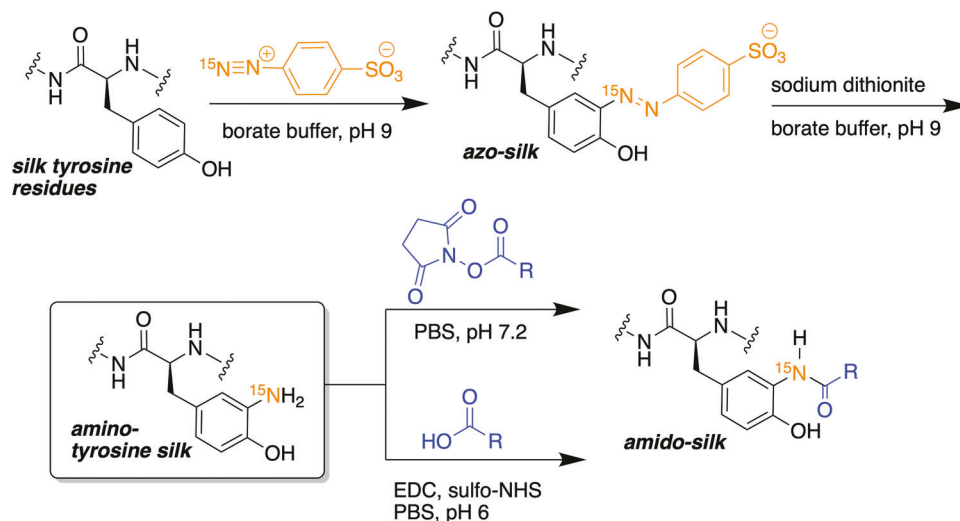
In the last decade, silk protein produced by *Bombyx mori* silkworms has emerged as one of the most versatile and highly studied biomedical materials. Raw silk fibers can be dissolved and re-processed into a variety of architectures including films, sponge-like scaffolds, hydrogels, microspheres, or re-spun into nanofibrous mats. The resulting materials have excellent biocompatibility, mechanical properties, and a slow degradation profile.<sup>[1,2]</sup> This versatility has allowed silk to be used extensively in biomedical applications such as 3D scaffolds for engineered tissues,<sup>[3,4]</sup> vessels for controlled drug delivery,<sup>[5,6]</sup> and biocompatible electronic devices.<sup>[7]</sup>

The heavy chain of native silk fibroin from *B. Mori* silkworms is a large protein containing 5263 amino acids, where >75% of the protein is composed of the nonreactive amino acids glycine and alanine.<sup>[8]</sup> The only reactive amino acids present in greater than 1 mol% are serine (12 mol%), tyrosine (5.3 mol%),

K. G. Hausken, R. L. Frevol, K. P. Dowdle, A. N. Young, J. M. Talusig, C. C. Holbrook, B. K. Rubin, A. R. Murphy  
 Department of Chemistry  
 Western Washington University  
 516 High St., Bellingham, WA 98225-9150, USA  
 E-mail: amanda.murphy@wwu.edu

 The ORCID identification number(s) for the author(s) of this article can be found under <https://doi.org/10.1002/macp.202200119>

DOI: 10.1002/macp.202200119



**Scheme 1.** General route to form an amide bond between activated esters and amino-tyrosine silk (isotopic label not required).

coupling but mitigates some of the drawbacks of the reaction. The general synthetic method used is outlined in **Scheme 1**. We demonstrate that under optimized conditions, 100% of the tyrosine residues can be converted to azo derivatives, and the azo groups can then be quantitatively reduced with sodium dithionite to produce tyrosines bearing a primary amine ortho to the hydroxyl group on the benzene ring (*o*-aminophenol, herein referred to as amino-tyrosine).<sup>[43,44]</sup> While the literature is sparse, further functionalization of peptides and proteins containing amino-tyrosine residues have been reported via reaction with activated carboxylic acids,<sup>[45,46]</sup> isothiocyanates,<sup>[47]</sup> aniline derivatives under oxidative conditions,<sup>[43,44]</sup> aldehydes via reductive amination,<sup>[48]</sup> or further diazonium coupling.<sup>[49]</sup> A related version of this modification has also been reported where *o*-aminophenol derivatives have been used to label the N-termini of proteins under oxidative conditions.<sup>[50]</sup> Here, we used activated carboxylic acids to modify the newly formed amine groups as these reactions are rapid, occur under mild conditions (room temp, pH 7.2), and there are a broad variety of commercially available carboxylic acid derivatives. To further demonstrate the utility of this reaction sequence, NHS-esters containing alkyne and azide functional groups were installed on the amino-tyrosine residues and bio-orthogonal copper-catalyzed azide-alkyne cycloaddition (CuAAC) and copper-free strain-promoted azide-alkyne cycloaddition (SPAAC) reactions were carried out with the alkyne- and azide-silk, respectively. To summarize, this reaction scheme provides improvements over the popular diazonium coupling method used to modify tyrosine residues in silk as it removes the highly colored azo group and can quantitatively install a nucleophilic amine on tyrosine which cannot be accomplished effectively with diazonium coupling reactions alone. The newly installed amine can be further elaborated with activated carboxylic acid derivatives, allowing conjugation of biomolecules or other molecules containing sensitive functional groups under very mild reaction conditions.

Silk is known to undergo some degradation during isolation and solubilization of the protein, so the resulting silk samples have a fairly broad range of molecular weights.<sup>[51]</sup> Due to the poly-

dispersity of the isolated silk, mass spectrometry and SDS-PAGE do not provide useful information regarding the extent of modification. Therefore, <sup>1</sup>H NMR, UV-vis, and FTIR were used as the primary methods of characterization. For further confirmation of each step of our reaction sequence, sodium nitrite labeled with <sup>15</sup>N (Na <sup>15</sup>NO<sub>2</sub>) was used to form the initial azo-silk, allowing the subsequent conversions to be followed with 2D <sup>1</sup>H-<sup>15</sup>N heteronuclear multiple bond correlation (HMBC) NMR experiments.

## 2. Results and Discussion

### 2.1. Synthesis of Amino-Tyrosine Silk

Previous works from our group have shown the diazonium coupling reaction to be an effective means for modifying the tyrosine residues in silk.<sup>[30,35]</sup> Theoretically any azo derivative could be used in this reaction scheme since the azo bond gets reduced in the second step. Here, we chose to use sulfanilic acid as the electron-withdrawing nature of the sulfonic acid aids in reactivity of the resulting diazonium salt. In addition, sulfanilic acid is water soluble, so the use of organic co-solvents can be avoided. Lastly, silk modified with sulfonic acids is stable in solution for long periods of time as the charged groups slow the natural gelation of the protein.<sup>[30,35]</sup>

Due to the high percentage of tyrosine residues in silk and the solubility limits of the diazonium salt, it was difficult to add enough diazonium salt in one aliquot to react with all of the tyrosine residues without effecting the pH or dramatically diluting the silk protein. Here, we found that an effective method to quantitatively convert all the tyrosine residues to azo groups was to perform the diazonium coupling reaction twice with a purification step in between. The resulting silk solution could be purified by dialysis or size-exchange chromatography, then concentrated as needed using a centrifugal concentrator. Alternatively, the silk protein could be diluted prior to reaction, and then reconcentrated for the subsequent steps. However, we found this method to be less reproducible, as we would often still have less than

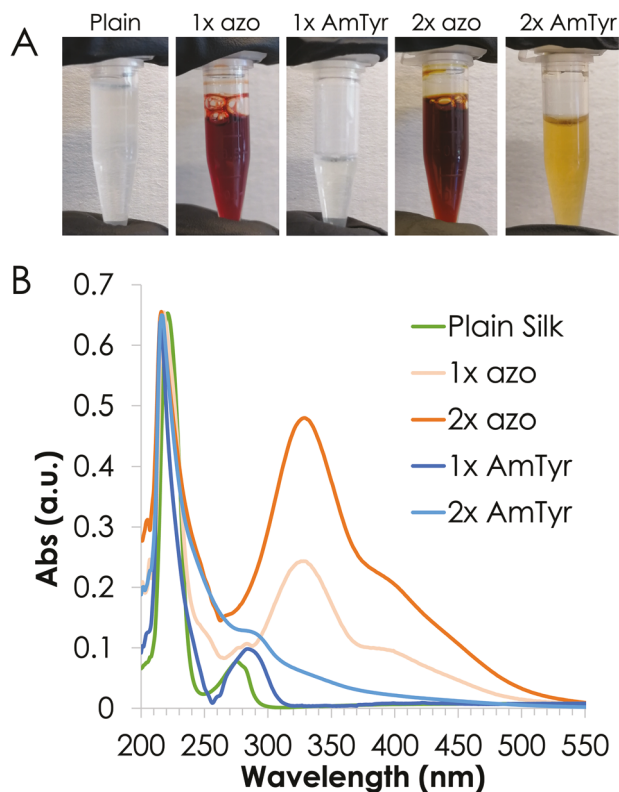


**Figure 1.** A) Photographs of the silk samples after the modifications listed, and B) the corresponding UV spectra (normalized to peak at 215 nm).

100% modification and would need to repeat the reaction twice anyway to ensure all of the tyrosines were modified.

Silk samples treated with the diazonium salt one time (1× azo-silk) had a dark red-orange color, while those reacted twice (2× azo-silk) were dark burgundy (Figure 1A). These azo-silk derivatives were then treated with excess sodium dithionite under basic conditions to reduce the azo bond to an amine, thus forming our major intermediate, amino-tyrosine silk (AmTyr-silk). An immediate color change was observed upon reduction, indicating loss of the azo bond (Figure 1A). The 1× AmTyr-silk samples were nearly colorless, but for some of the 2× AmTyr-silk samples, the solutions were pale yellow and did not lighten even with further equivalents of dithionite or longer reaction times. As discussed further below, evidence of bis-azo formation in the 2× azo-silk samples was observed in some NMR spectra, which may have resulted in darker solutions after reduction (structures of potential by-products are shown in Figure S1, Supporting Information). These reactions are also carried out at high pH, making it possible for the diazonium salt to form triazine linkages with the few lysine side chains in silk or the N-termini (Figure S1, Supporting Information).<sup>[52]</sup> Triazines are typically yellow in color and have been shown to be resistant to reduction, which could be the cause of the residual color in the silk solutions. However, we have been unable to find any other direct evidence of triazines in the 2× azo-silk samples and subsequent derivatives, so it is unlikely to be forming in an appreciable amount. Attempts to perform the reaction at lower pH to suppress any potential triazine formation

were unsuccessful, as azo conversion was low and the silk tended to solidify into a gel either during reaction or purification.

The formation and subsequent loss of the azo bond was further confirmed with UV-vis spectroscopy (Figure 1B). The 2× azo-silk had a higher relative absorbance at 330 nm for the azo group than the 1× azo-silk sample, further supporting that the modification was incomplete after the first round of reaction. After reduction of the 1× azo-silk, the azo absorbance was completely gone. In addition, the tyrosine absorbance was found to shift from the 278 nm observed for plain silk to 290 nm, consistent with the effect of adding a new amino group to the aromatic ring. After reduction of the 2× azo-silk, the azo peak diminished greatly, but there was still some background absorbance from 300 to 450 nm, which is consistent with the visible yellow coloring of the sample.

As expected, the AmTyr-silk derivatives were not very stable over time as the electron-rich amino-tyrosine rings are susceptible to oxidation. Solutions of the 2× AmTyr-silk were found to turn brown over a few days (Figure S2A, Supporting Information). While the color change was visible to the eye, no obvious change was detected in the UV-vis spectra within the first few days. By two weeks, however, the peak at 290 nm became less pronounced and the background absorbance from 300 to 500 nm increased slightly (Figure S2B, Supporting Information). The NMR spectra were also unchanged for brown-colored samples stored for a few days, but after a few weeks the aromatic regions became blurred (data not shown). As the azo-silk is very stable and the reduction reaction is rapid (30 min) the recommended procedure is to reduce the azo-silk and complete any subsequent reactions on the same day. Alternatively, we found that the AmTyr-silk was stable for months if stored under refrigeration with sodium dithionite in the solution to prevent oxidation. The reducing reagent could then be removed using disposable size-exclusion columns just prior to use.

## 2.2. <sup>1</sup>H NMR of Azo- and Amino-Tyrosine Silk

The reaction products at each step were characterized using NMR. Disposable size-exclusion columns were used to exchange silk into D<sub>2</sub>O prior to analysis. Figure 2 shows the aromatic region of the <sup>1</sup>H NMR spectra of plain silk, azo-silk and AmTyr-silk derivatives (full spectra are given in Figures S3–S5, Supporting Information). Following the diazonium reaction, signals for the new aromatic rings in the azo group appear downfield at ≈7.8–7.9 ppm, consistent with previous works.<sup>[30]</sup> The presence of native tyrosine resonances were difficult to clearly discern in the azo-silk samples, but the peaks in the 6.8 and 7.1 region are much broader in the 1× azo-silk sample as compared to the 2× azo-silk sample, suggesting that there was still some unmodified tyrosine. After reduction, the aromatic signals for the azo group are completely gone and three distinct peaks appear between 6.4 and 6.8 ppm that are consistent with the predicted C—H resonances on the amino-tyrosine ring. Peaks corresponding to both the unmodified tyrosine and the amino tyrosine rings can be readily distinguished in the 1× AmTyr-silk sample, whereas no native tyrosine signals remain in the 2× AmTyr-silk sample, signifying complete modification of all the tyrosine rings. From the relative integration values of the aromatic peaks in the 1× AmTyr-silk sample (Figure S5A, Supporting Information), ≈65% of the

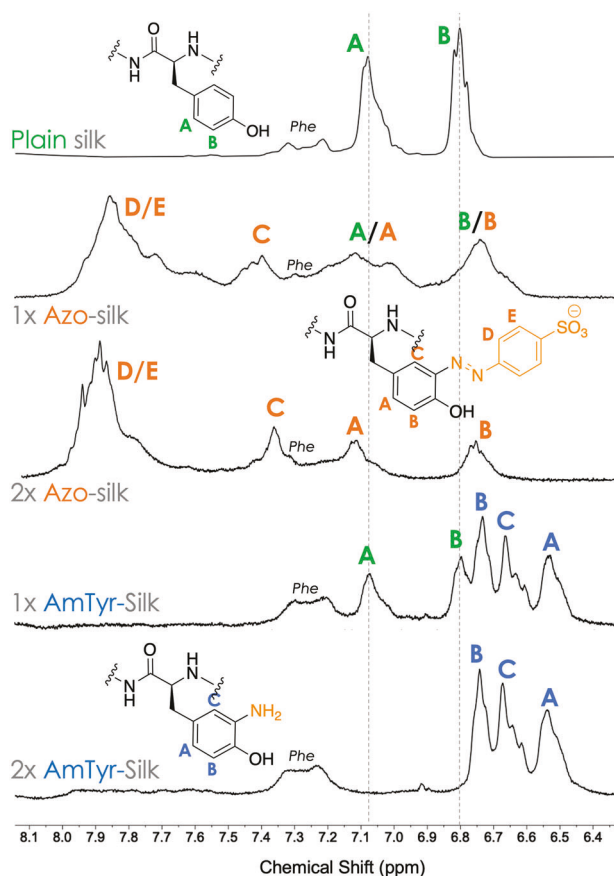


**Figure 2.** Expansion of the aromatic region of the  $^1\text{H}$  NMR spectra of plain silk and silk derivatives modified as noted ( $\approx 1\text{--}3$  wt% silk in  $\text{D}_2\text{O}$ ). Full spectra are given in Figures S3–S5 (Supporting Information).

tyrosine residues were modified ( $\approx 180$  per silk molecule) in the first round of the diazonium reaction. In some 2 $\times$  azo-silk samples, a peak at 7.65 ppm was observed (Figure S6, Supporting Information) and was attributed to tyrosine residues with two azo groups, a by-product formed due to the addition of excess diazonium salt. Following reduction of these samples, a corresponding peak at 6.19 ppm in the 2 $\times$  AmTyr-silk spectra was observed which is consistent with the expected resonance for a tyrosine bearing two amine groups (Figure S6, Supporting Information).

### 2.3. Amidation of Amino Tyrosine

The new amine group on tyrosine could be further elaborated using standard amidation reactions with commercially available carboxylic acids or NHS-ester derivatives under very mild conditions (Scheme 2). For these proof-of-concept experiments, an amidation reaction was used to install bio-orthogonal alkyne and azide groups that can selectively react with azides and alkynes, respectively. These amidation reactions should also modify the native lysine residues in silk, but the low abundance of lysine (0.2 mol%, 12 per protein) relative to tyrosine (5.3 mol%, 277 per protein)<sup>[8]</sup> makes that product insignificant.

The 2 $\times$  AmTyr-silk derivatives with no unmodified tyrosine remaining were used for these experiments to simplify the  $^1\text{H}$

NMR analysis of the products. To produce alkyne-labeled silks, a carbodiimide coupling reaction with 4-pentynoic acid (Scheme S1, Supporting Information) was first compared to a reaction utilizing an alkyne containing an NHS-ester (Scheme 2). Both methods were successful at forming a new amide bond to the amino-tyrosine ring ( $^1\text{H}$  NMR of both products provided in Figures S7 and S8A, Supporting Information). However, the NHS-ester became the method of choice for further experiments as it introduced less by-products into the sample and avoids potential crosslinking reactions with the native carboxylic acids in silk.

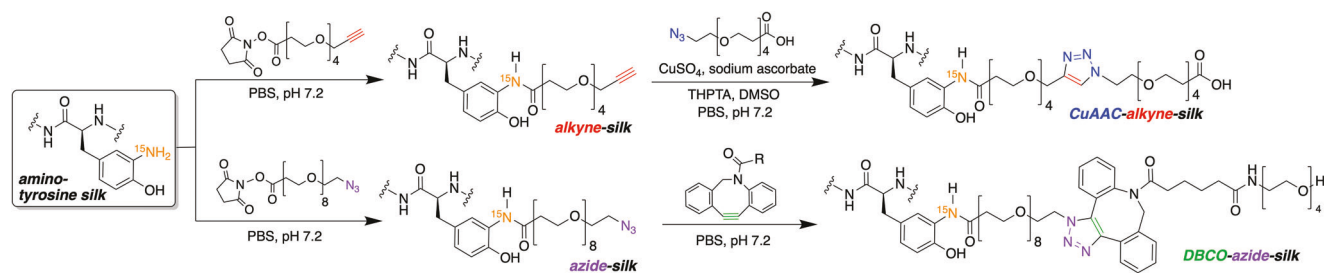
Using this very mild reaction (room temperature, pH 7.2), the amino-tyrosine groups could be modified in nearly quantitative yield using  $\approx 4\text{--}5$  equivalents of the NHS-ester relative to the number of tyrosine residues to produce silk derivatives with both alkyne and azide functionality. NHS-esters containing poly(ethylene glycol) (PEG) linkers were used so that the reactions could be carried out in buffer without the need for a co-solvent. Following reaction, dialysis was found to be the most effective purification method to remove any unreacted NHS-ester.

As shown in Figure 3, the three peaks corresponding to the aromatic resonances on the amino-tyrosine ring at 6.5–6.8 ppm were almost completely absent for alkyne-silk and azide-silk. On occasion, the products had hints of the AmTyr peaks remaining, but they were difficult to clearly discern. For both derivatives, a new set of aromatic peaks between 6.8 and 7.5 ppm appeared which were consistent with predicted values for a tyrosine bearing an amide group ortho to the hydroxyl. Both derivatives had peaks corresponding to the ethylene glycol repeats  $\approx 3.5$  ppm (\*) and a new peak at 2.7 ppm (#) that was assigned to the methylene protons adjacent to the amide carbonyl (full peak assignments in Figures S8 and S9, Supporting Information; further discussion in the HMBC section below). Unique peaks that corresponded to the methylene protons adjacent to the alkyne at 4.2 ppm (1) and the terminal alkyne proton at 2.8 ppm (2) were readily discernable in the alkyne-silk spectrum (full peak assignments in Figure S8, Supporting Information). Likewise, the methylene protons next to the  $\text{—N}_3$  group had a distinct signal at 3.4 ppm (6) in the azide-silk spectrum (full peak assignments in Figure S9, Supporting Information). While the assembly state of the silk protein in solution could affect the results, the relative integration values suggest that  $\approx 80\text{--}100\%$  of the tyrosine residues were converted to the amide derivatives.

### 2.4. Bio-orthogonal Conjugation Reactions

To further demonstrate the potential of this reaction sequence, bio-orthogonal CuAAC and SPAAC reactions were carried out with the alkyne- and azide-silk, respectively. Both reactions were conducted at room temperature in phosphate buffered saline (PBS) buffer at pH 7.2.

The reaction between alkyne-silk and azide-PEG<sub>4</sub>-acid (Scheme 2) was catalyzed by  $\text{CuSO}_4$  reduced in situ by sodium ascorbate. In addition, tris(3-hydroxypropyltriazolylmethyl)amine (THPTA) was added to serve as a ligand for the copper.<sup>[53]</sup> Following purification via dialysis, the  $^1\text{H}$  NMR spectrum (Figure 3 and Figure S8b, Supporting Information) revealed that the peaks corresponding



**Scheme 2.** Amidation reactions carried out with AmTyr-silk to produce alkyne- and azide-silk and the products after subsequent CuAAC and SPAAC reactions.

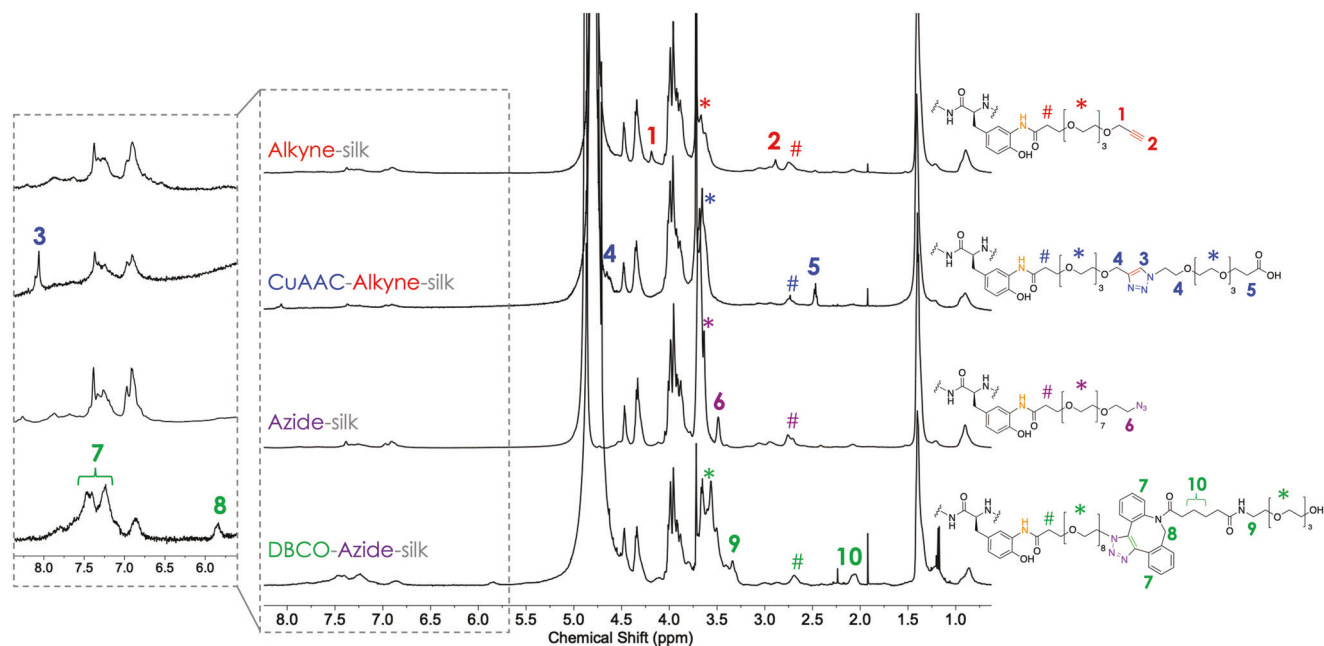


**Figure 3.** Comparison of the  $^1\text{H}$  NMR spectra of the silk derivatives ( $\approx 1$  wt% silk in  $\text{D}_2\text{O}$ ). NHS amidation reactions were carried out using  $2\times$  AmTyr-silk. An expansion of the aromatic regions is given for clarity. Peaks confirming the newly installed groups are highlighted, while full peak assignments for all spectra are given in Figures S8 and S9 (Supporting Information).

to the methylene protons adjacent to the alkyne and the terminal alkyne proton were gone (1 and 2 in Figure 3). In addition, new peaks appeared that were consistent with predicted spectra of the triazole product, including a peak at 8.0 ppm (3) for the proton on the triazole ring, the methylene protons adjacent to the triazole ring at 4.6 ppm (4, on the shoulder of the water peak), an increase in the ethylene glycol resonances  $\approx 3.5$  ppm (\*) and the methylene adjacent to the terminal carboxylic acid at 2.5 ppm (5). While the broad NMR signals preclude exact quantification, the extent of conversion was estimated to be between 70% and 100%. The lack of remaining alkyne peaks imply that the reaction reached full conversion, but some residual signals from the alkyne could be masked by adjacent resonances. The relative integrations of the new peaks suggest that  $\approx 70\%$  of the alkyne groups were modified (Figure S8b, Supporting Information).

The SPAAC reaction between azide-silk and DBCO-PEG<sub>4</sub>-alcohol (Scheme 2) was also deemed successful. This reaction could be monitored in real time using UV, as the DBCO group has a characteristic absorbance at 309 nm which disappears fol-

lowing cycloaddition with an azide.<sup>[54]</sup> In initial trials, the reaction was run on a small scale with either a sub-stoichiometric amount of the DBCO reagent ( $\approx 0.04$  eq. relative to tyr) or excess DBCO ( $\approx 2$  eq. relative to tyr) in a 96-well plate and monitored periodically with a plate reader. In the sub-stoichiometric reaction, the majority of the DBCO reacted in  $\approx 2$  h as evidenced by a sharp decrease in absorbance at 309 nm, although the peak continued to decrease slightly over a 24 h period (Figure S10A, Supporting Information). When excess DBCO-PEG<sub>4</sub>-alcohol was added, the DBCO absorbance initially decreased, but leveled off after  $\approx 4$  h indicating that all available azides in the silk were consumed (Figure S10B, Supporting Information). For the larger scale reactions, an excess of the DBCO reagent was used to ensure high conversions ( $\approx 2$  eq. relative to tyrosine). Following purification using disposable size-exclusion columns, the products were analyzed with UV and  $^1\text{H}$  NMR. The UV spectrum of the product was distinct from the azide-silk starting material, with a broad featureless absorption between 270 and 320 nm (Figure S10, Supporting Information). Notably, the purified DBCO-silk product

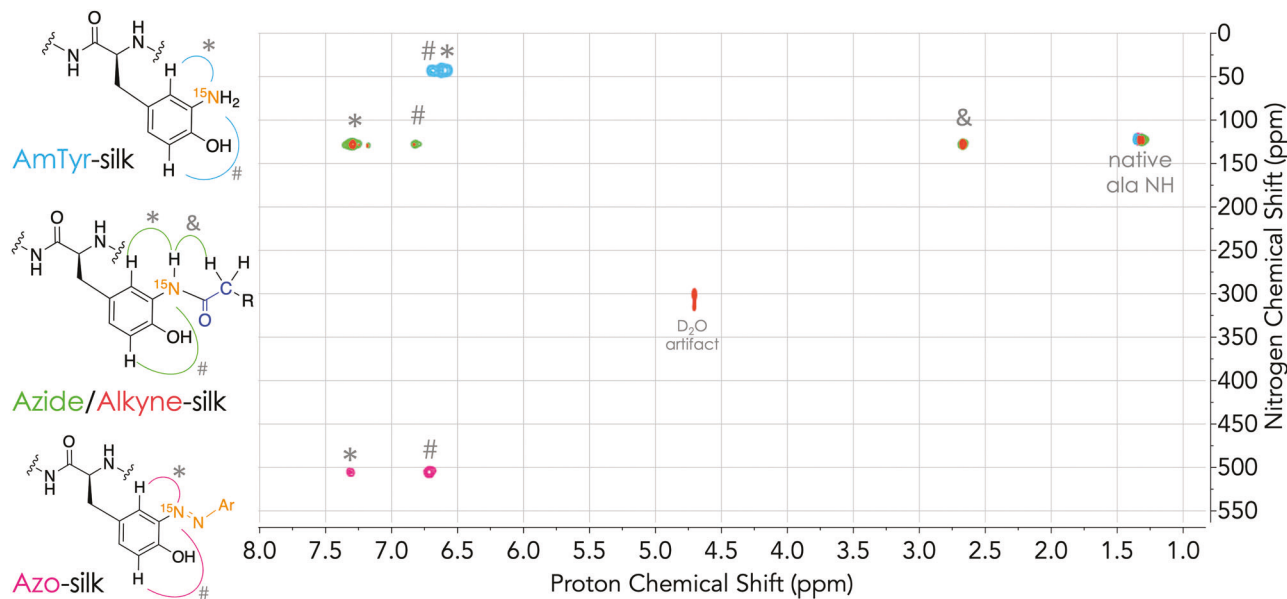


**Figure 4.** Overlaid contour plot of the 2D  $^1\text{H}$ - $^{15}\text{N}$  HBMBC NMR spectra of  $^{15}\text{N}$ -labeled azo-silk (magenta), AmTyr-silk (blue), alkyne-silk (orange), and azide-silk (green). Individual spectra can be found in Figures S11–S14 (Supporting Information).

spectrum was nearly identical to the 24 h time point from the stoichiometric small-scale reaction, where the peak at 309 nm was completely gone. This indicated that size exclusion was effective at removing the excess unreacted DBCO starting material from the large-scale reaction. As highlighted in Figure 3, evidence of reaction could also be seen using  $^1\text{H}$  NMR. New peaks assigned to the alkyl linkers in the DBCO reagent appeared at 2.1 (10) and 3.3 ppm (9), an increase in the ethylene glycol resonances  $\approx 3.5$  ppm (\*) was noted, and peaks for the methylene protons in the cyclic core of the DBCO reagent were found at 5.8 ppm (8) (see full peak assignments in Figure S9B, Supporting Information). Additional peaks corresponding to the new aromatic rings were also present but overlapped with the existing tyrosine resonances (7).

## 2.5. 2D $^1\text{H}$ - $^{15}\text{N}$ HBMBC Spectroscopy of Modified Silks

To allow for complementary 2D NMR characterization of the modification sequence, isotopically labeled  $\text{Na } ^{15}\text{NO}_2$  was used to form the diazonium salt in the initial diazonium reaction. When the labeled diazonium salt reacts with tyrosine, the isotopic nitrogen becomes directly attached to the phenol ring and this labeled nitrogen atom remains following reduction and any subsequent functionalization (Scheme 1). The fate of the  $^{15}\text{N}$  label can then be followed using 2D  $^1\text{H}$ - $^{15}\text{N}$  HBMBC spectroscopy, as the chemical shift of the nitrogen and the corresponding proton cross peaks are unique for each product in the reaction sequence. For HBMBC, cross peaks between a nitrogen and protons up to four bonds away are commonly observed.

An overlaid plot of the HBMBC data from representative azo-silk, AmTyr-silk, alkyne-silk, and azide-silk samples is provided in Figure 4. Full spectra with peak assignments of plain silk and the individual silk derivatives can be found in Figures S11–S14 (Supporting Information).

For plain silk prior to modification, cross peaks between the naturally abundant  $^{15}\text{N}$  in the native amide nitrogen atoms and the alpha and beta protons in alanine, the alpha and beta protons in serine and the alpha protons in glycine were observed (Figure S11, Supporting Information). While information on the secondary structure of the silk protein was not the focus of these experiments, the chemical shifts of the  $^{15}\text{N}$  atoms matched reported values for these amino acids in a random coil protein structure.<sup>[55]</sup> The cross peak with the alanine beta protons had the strongest signal, and this peak was also observed in all of the modified derivatives ( $^1\text{H}$  @ 1.4 ppm;  $^{15}\text{N}$  @ 123.1 ppm).

As shown in Figure 4, a cross peak between the  $^{15}\text{N}$  in the azo bond at 505 ppm and the ortho aromatic proton at  $\approx 7.3$  ppm was observed in all azo-silk spectra (full spectrum given in Figure S12, Supporting Information). Some, but not all, azo-silk samples had an additional cross peak between the azo  $^{15}\text{N}$  and the meta aromatic proton at  $\approx 6.7$  ppm. The chemical shift of the nitrogen was consistent with an azo bond,<sup>[56]</sup> further confirming the modification. After reduction of the azo-silk to AmTyr-silk, the peak corresponding to the azo  $^{15}\text{N}$  was gone, and was replaced by a signal with a chemical shift of 43–44 ppm, consistent with a primary amine or aniline (Figure 4 and Figure S13, Supporting Information).<sup>[56]</sup> The  $^{15}\text{N}$  had a strong cross signal with the ortho proton on the tyrosine peak at 6.67 ppm and a weaker cross signal with the meta proton at 6.74 ppm. In some of the 2 $\times$  AmTyr-silk samples, we also observed a proton resonance at 6.20 ppm that had a cross peak with a  $^{15}\text{N}$  with a chemical shift of 45 ppm (Figure S13B, Supporting Information). As discussed earlier, we attribute this to bis-amino tyrosine that was generated from tyrosine residues with two azo groups attached before reduction (Figure S1, Supporting Information).

As expected, the HBMBC spectra for alkyne-silk and azide-silk were nearly identical given the similarity in structure (Figure S14, Supporting Information). For both derivatives, the amino-tyrosine  $-\text{NH}_2$  peaks at  $\approx 44$  ppm were gone after reaction with

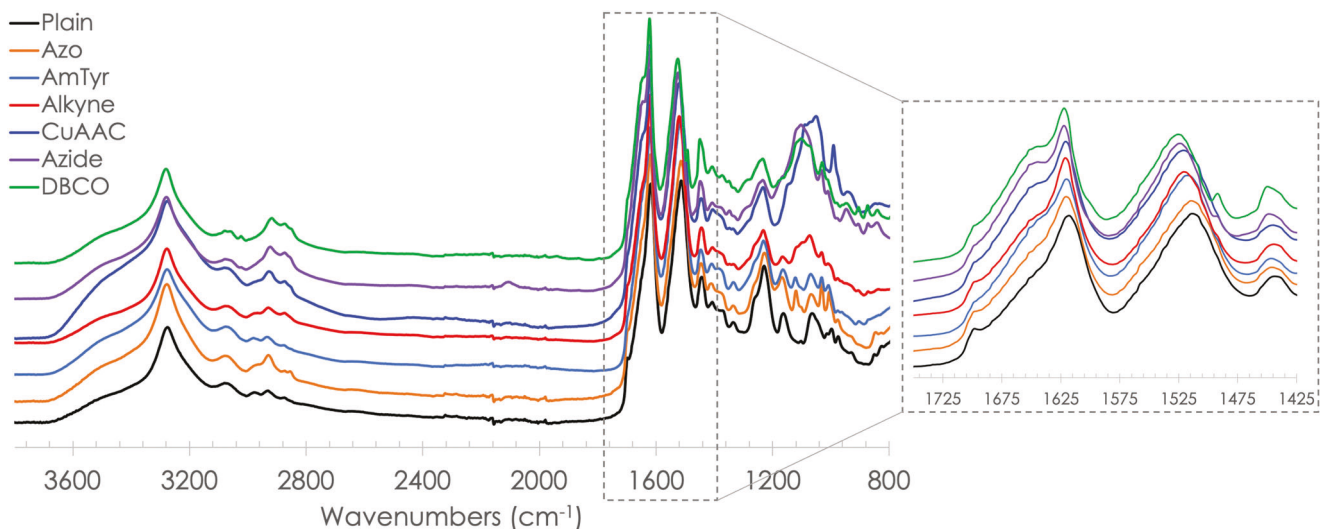


**Figure 5.** ATR-FTIR spectra of the silk derivatives noted. Films were cast, dried, and crystallized by exposure to methanol prior to analysis.

≈4–5 equivalents of the NHS-esters. In some cases where less equivalents were used, small peaks for residual AmTyr-silk could be discerned (Figure S14B, Supporting Information). In addition, new  $^{15}\text{N}$  signals at ≈127–129 ppm appeared, consistent with the chemical shift of an amide nitrogen (Figure 4).<sup>[56]</sup> These amide  $^{15}\text{N}$  signals had a strong cross peak with the ortho protons on the tyrosine at 7.3 ppm and a weaker cross peak with the meta protons at 6.8 ppm (Figure 4 and Figure S14, Supporting Information). Both derivatives also showed a strong cross peak with the resonance assigned to the methylene protons adjacent to the newly installed amide carbonyl ( $^1\text{H}$  @ 2.6 ppm;  $^{15}\text{N}$  @ 127 ppm), further confirming that the amide bond formation was successful. The CuAAC-alkyne-silk or the DBCO-azide-silk was not evaluated with this technique as no further changes to the isotopically labeled nitrogen occur during these reactions.

## 2.6. FTIR Analysis of Modified Silks

Silk is known for its robust mechanical properties, which have been attributed to the fact that the protein self-assembles into a highly crystalline beta-sheet structure.<sup>[8]</sup> One method that has been used extensively to track the assembly of silk has been FTIR, as the amide carbonyl stretch (“amide I” stretch) is sensitive to the extent of hydrogen bonding and thus the vibration can be correlated to different silk conformations (random coil vs beta sheet).<sup>[57]</sup> While silk can spontaneously crystallize, exposure to organic solvents, stress or heat have been shown to rapidly induce the transition from a soluble, random coil structure to a water-insoluble beta sheet structure. This transition has been characterized previously with FTIR, where the random coil conformation of silk typically shows a broad amide I stretch centered ≈1650  $\text{cm}^{-1}$ , whereas silk in a primarily beta sheet conformation shows a sharper amide I stretch at ≈1620  $\text{cm}^{-1}$ .<sup>[57]</sup>

The ATR-FTIR spectra of all silk derivatives synthesized here are provided in the overlaid plot in **Figure 5**. For reference, a spectrum of plain silk before modification is also provided. Solutions of each silk derivative were cast in weigh boats, dried in an oven

and then treated briefly with methanol to induce crystallization. All derivatives exhibit a prominent amide I stretch at 1620  $\text{cm}^{-1}$ , indicating that a significant fraction of all of the modified silk proteins is able to crystallize into a beta sheet structure. However, for the CuAAC-silk, azide-silk, and DBCO-silk derivatives, a shoulder at 1650  $\text{cm}^{-1}$  was clearly visible. Likewise, the “amide II” peak at 1510  $\text{cm}^{-1}$  corresponding to the N–H bend and C–N stretch also shifted to slightly higher wavenumbers (1525  $\text{cm}^{-1}$ ) as the modifications increase in size. These two observations indicate that the derivatives containing the largest substituents are unable to achieve the same extent of beta-sheet conformation as the unmodified protein. However, each of these derivatives also contain new amide bonds that are part of the linker groups, so it is possible that the shoulder observed is partly due to those overlapping bond vibrations. While mechanical testing was outside the scope of the experiments presented here, for applications where the mechanical properties of silk must be fully preserved, an alternative would be to carry out the modifications on the surface of solid silk structures as described in the section below.

As expected with the derivatives containing PEG linkers, new C–O stretches at ≈1150  $\text{cm}^{-1}$  and an increase in the C–H intensity ≈2900  $\text{cm}^{-1}$  were observed in the alkyne-silk, CuAAC-silk, azide-silk, and DBCO-silk derivatives. The azide-silk spectra also contained a small broad peak at 2100  $\text{cm}^{-1}$  corresponding to the  $-\text{N}_3$  group, but we did not observe distinct vibrations corresponding to the carbon–carbon triple bond or sp C–H groups in the alkyne-silk derivatives.

## 2.7. Modification of Solid Silk Structures

All of the reactions described above were carried out on solubilized silk proteins to maximize the extent of tyrosine modification. However, these methods can be readily adapted to chemically modify solid forms of silk if desired. Here, only the portion of the protein exposed to the reaction solution will be modified, but the architecture and mechanical integrity of the silk structure can be preserved throughout the mild reaction sequence. To

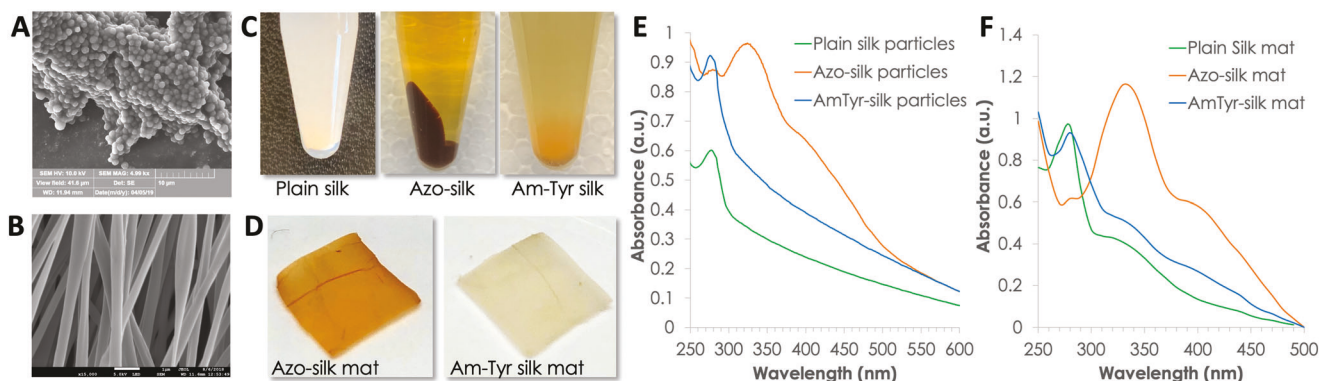


**Figure 6.** SEM images of A) representative silk microparticles and B) electrospun silk mat with aligned fibers used in this study. Photographs of C) silk microparticles during reaction and D) silk electrospun mats after modification ( $3 \times 3$  cm) showing the color changes observed with surface modification. UV spectra of E) silk particles and F) electrospun mats before and after modification. The mats were thin enough to collect the UV spectra directly through the mats using a plate reader but the particles were dissolved in 9.3 M LiBr prior to analysis.

demonstrate the method with representative forms of silk, microparticles and electrospun mats were subjected to the entire reaction sequence and reaction progress of the first two steps was followed visually and with UV (Figure 6). Silk microparticles and aligned electrospun silk mats were produced using established protocols,<sup>[58,59]</sup> and SEM was used to verify the initial structures (Figure 6A,B). The modification reactions were carried out in an analogous manner to the solution reactions where the only difference was that the solid particles and mats were suspended in buffer for each step, rather than being dissolved. The solid nature of the samples also facilitated purification as they could simply be rinsed to wash out excess reagents and byproducts.

Silk microparticles showed the same color progression as that observed in solution (Figure 6C) where the particles went from white to dark red during the azo coupling, then lightened to yellow during reduction. No further changes in color were noted following the NHS reactions. Electrospun mats also had visual changes, but the colors are more muted as the mats are very thin (Figure 6D). UV was used to further characterize the progression from azo-silk to AmTyr-silk (Figure 6E,F). While the electrospun mats were thin enough for direct UV measurements using a plate reader, the absorption peaks for the solid particles were broad and ill-defined to the opacity of the particles. Therefore, to obtain better spectra, the modified microparticles were dissolved in LiBr, diluted into PBS and the UV spectra were recorded using a plate reader. Regardless of the sample preparation method, all samples exhibited the characteristic azo absorption at 330 nm, which disappeared following reduction. No further visible color changes or changes to the UV spectra were observed when the AmTyr-silk particles or mats were reacted with the NHS-esters. Likewise, no discernable differences in the solid silk samples were observed in SEM after the reaction sequence was completed.

### 3. Conclusion

Here, a reaction sequence was developed that can be used to quantitatively modify the tyrosine residues in silk. Conversion of the native tyrosine rings to azobenzene, followed by reduction of the azo bond results in an electron-rich amino-tyrosine group

that can be acylated under mild conditions that are suited for a wide variety of carboxylic acid or NHS-ester derivatives. The intermediate reduction step provides advantages over using the diazonium coupling reaction alone, as it generates a nucleophilic amine which cannot be directly installed via diazonium chemistry and the highly colored azo group is removed. A unique method to follow this reaction sequence using isotopically labeled reagents and 2D NMR spectroscopy was also employed. These reactions can be carried out on silk samples dissolved in buffer, or on solid silk substrates such as films, 3D scaffolds, fibers, etc. Further work is underway to use this chemistry to attach sensitive biomolecules to silk for drug delivery, tissue adhesives and tissue engineering applications, as well as explore other reactive pathways for the amino-tyrosine intermediate.

### 4. Experimental Section

**Materials:** All chemicals, unless otherwise stated, were purchased from Sigma-Aldrich, BroadPharm, Acros, J.T. Baker, Alfa Aesar, Mallinckrodt Chemicals or Fisher Scientific and were used without further purification. *B. mori* silk cocoons were purchased from Oregon Silkworms in Bend, OR. Nanopure (NP) water used in buffers or reactions was purified using a Millipore Milli-Q Advantage A10 purification system.

**Instrumentation:** All NMR spectra were obtained using a Bruker Avance III 500 MHz instrument, using deuterium oxide as the solvent. Data analysis and  $^1\text{H}$  NMR predictions were carried out using MestReNova software (v14). UV-vis data were collected with a Jasco V-670 UV-vis spectrophotometer or a BioTek Synergy H1MF model plate reader in PBS buffer or water. Electrospinning was performed using a Spraybase electrospinning instrument with a rotating drum collector by Profector Life Sciences Ltd. The entire instrument was contained in a custom-built polycarbonate chamber to control the humidity.

**Preparation of Aqueous Silk Solution:** *B. mori* cocoons (10) were cut up into small pieces and scattered in a rapidly boiling aqueous solution of 0.02 M  $\text{Na}_2\text{CO}_3$  (1.5 L). The beaker was covered with aluminum foil and the solution was boiled for 1 h while stirring. The fibers were removed, pulled apart and placed in 1 L of rapidly boiling nanopure water for 10 min. The rinsing procedure was repeated three more times using rt water and then the fibers were spread out and dried overnight in a fume hood. The dry fibers were weighed, placed into a 200 mL beaker, and covered with an aqueous solution of 9.3 M LiBr (5 mL of LiBr per 1 g silk). The beaker was covered with aluminum foil and put into a 60 °C oven until dissolved (45 min to 1 h). The resulting solution was transferred to dialysis tubing

(Fisher Brand, 3500 MWCO) and dialyzed against 3 L of DI water for 1 h. The water was changed and dialyzed for another 3 h. After 3 h, the water was changed again and left to dialyze overnight. The resulting solution was filtered through a syringe containing a polypropylene frit (Torvliq #SF-5000) to remove any remaining dust and debris from the cocoon.

For further reactions on the silk protein in solution, following the dialysis against water described above, the dialysis tube was placed in borate buffered saline (BBS,  $100 \times 10^{-3}$  M borate,  $137 \times 10^{-3}$  M NaCl, pH 9–9.4) and left overnight. The dialysis tube was then transferred to a fresh buffer solution and dialyzed for another 8 h. Silk solutions were stored under refrigeration until further use.

**Silk Molarity Calculations:** Silk is known to degrade during the purification and solubilization process leading to a dispersity in molecular weight that makes the reagent calculations imprecise. To estimate the amounts of reagents needed for each reaction, the molar ratios reported below were calculated assuming the full molecular weight of silk (391 kDa) and the fact that silk contains 5.3 mol% tyrosine (277 tyr residues per protein). The concentration ( $\text{mg mL}^{-1}$ ) of silk solutions was determined by drying aliquots of the solution in an oven at  $60^\circ\text{C}$  for at least 1 h and weighing the residual protein.

**Diazonium Coupling Reaction:** Silk solution (16 mL, 3–4% w/v,  $\approx 1.4 \times 10^{-3}$  mmol silk;  $\approx 4 \times 10^{-1}$  mmol tyr) in BBS was placed in a 50 mL Falcon tube and cooled on ice. The diazonium salt was prepared by combining sulfanilic acid (69 mg, 0.4 mmol) and *p*-toluene sulfonic acid monohydrate (*p*-TSA, 304 mg, 1.6 mmol) in 4 mL DI water. The solution was placed in a water bath sonicator until dissolved and then cooled on ice.  $\text{NaNO}_2$  (4 M solution in water, 100  $\mu\text{L}$ , 0.40 mmol) was added to the sulfanilic acid solution, inverted to mix, and returned to ice for 15 min. The resulting diazonium salt solution was combined with the chilled silk solution, inverted to mix, and left to react for 40 min on ice. The resulting dark red solution was pipetted into a hydrated dialysis tube and dialyzed against 1 L DI water, then against 1 L BBS, changing the buffer twice over a period of 24 h. To obtain quantitative labeling of the tyrosine groups, this reaction was repeated a second time using the same reaction and purification conditions. The resulting solution was concentrated to  $\approx 4\%$  w/v using a centrifugal concentrator (Cytiva Vivaspin 6, 20k MWCO), or by laying the dialysis bag on a bed of dry polyethylene glycol powder (12k) for several hours. These azo-silk solutions were stored under refrigeration until further use.

Isotopically labeled azo-silk was prepared in the same manner, but with labeled  $\text{Na}^{15}\text{NO}_2$  (>98%, Cambridge Isotope Laboratories, Inc.). The solid  $\text{Na}^{15}\text{NO}_2$  reagent was dissolved in NP water to make a 4 M solution and then used in an identical fashion to that described above.

**Reduction of Azo to Amino-Tyrosine:** *Caution:* Sodium hydrosulfite may decompose upon exposure to air and moisture and may liberate toxic gas if exposed to acid. Sodium hydrosulfite ( $\text{Na}_2\text{S}_2\text{O}_4$ , 127 mg, 0.73 mmol) was added in three portions to 1 $\times$  or 2 $\times$  azosilk solution in BBS (1.0 mL,  $\approx 4\%$  w/v,  $\approx 1.0 \times 10^{-4}$  mmol silk;  $\approx 2.8 \times 10^{-2}$  mmol tyr), vortexing after each addition (clumps if added all at once). The solution was left to react for 30 min. The mixture was then purified by passing through a size exclusion column (NAP-10, Cytiva) equilibrated with PBS ( $100 \times 10^{-3}$  M phosphate,  $150 \times 10^{-3}$  M NaCl, pH 7.2) or  $\text{D}_2\text{O}$  for NMR analysis. The resulting AmTyr-silk solutions were used immediately whenever possible or stored under refrigeration until further use (turns brown over time).

**Carbodiimide Coupling:** To attach alkyne groups to the silk, 1 mL of 2 $\times$  AmTyr-silk in PBS ( $\approx 2\%$  w/v,  $\approx 5 \times 10^{-5}$  mmol silk;  $1.4 \times 10^{-2}$  mmol tyr) was combined with 4-pentynoic acid (7.1 mg, 72  $\mu\text{mol}$ ), N-hydroxysulfosuccinimide sodium salt (sulfo-NHS) (15.6 mg, 72  $\mu\text{mol}$ ), and 1-ethyl-3-(3-dimethylaminopropyl)carbodiimide (EDC, 13.8 mg, 89  $\mu\text{mol}$ ). The solutions were vortexed to mix and left to react for 2 h at rt. The solutions were then purified by passing through size exclusion columns (NAP-10, Cytiva) equilibrated with either PBS for further reaction or  $\text{D}_2\text{O}$  for NMR.

**Reaction with NHS-Esters:** Propargyl-PEG<sub>4</sub>-NHS ester (BroadPharm #BP-21612) (23 mg, 64  $\mu\text{mol}$ ) or azido-dPEG 8-NHS ester (Sigma-Aldrich #QBD10503, 35 mg, 62  $\mu\text{mol}$ ) was added to a microcentrifuge tube containing 1 mL of freshly prepared 2 $\times$  AmTyr-silk in PBS ( $\approx 2\%$  w/v,  $\approx 5 \times 10^{-5}$  mmol silk;  $1.4 \times 10^{-2}$  mmol tyr). The mixture was left to react at rt for 3 h, vortexing periodically. The solutions were then purified by dialyzing

against 1 L PBS for  $\approx 24$  h (ThermoFisher Scientific Slide-A-Lyzer G2 dialysis cassette, 20 kDa MWCO). The solution was centrifuged at 4000 rpm for 15 min in a pre-rinsed spin concentrator (Cytiva Vivaspin, 10 kDa) to concentrate the solution as needed. For NMR, 0.5 mL of the purified solutions was passed through a NAP-5 column equilibrated with  $\text{D}_2\text{O}$ .

**CuAAC Reaction with Alkyne-Silk:** In an Eppendorf tube, alkyne-silk (1 mL,  $\approx 1\%$  w/v,  $\approx 2.5 \times 10^{-5}$  mmol silk;  $\approx 7.0 \times 10^{-3}$  mmol tyr) in PBS was combined with azido-PEG<sub>4</sub>-acid (BroadPharm #BP-20517) (13 mg, 45  $\mu\text{mol}$ ) and vortexed to mix. In a separate Eppendorf tube, tris(3-hydroxypropyltriazolylmethyl)amine (THPTA, 39 mg, 90  $\mu\text{mol}$ ) and copper sulfate ( $\text{CuSO}_4$ , 6.0 mg, 38  $\mu\text{mol}$ ) were dissolved in 100  $\mu\text{L}$  DMSO, and vortexed to mix. The two mixtures were combined, and the orange solution turned dark green. Sodium-L-ascorbate (14.6 mg, 74  $\mu\text{mol}$ ) was then added to the combined mixture and vortexed to mix. The green solution immediately became orange once again. The solution was left to react for 3 h at rt. The solution was dialyzed (ThermoFisher Scientific Slide-A-Lyzer G2 dialysis cassette, 10 kDa) against PBS for 24 h. An aliquot (0.5 mL) was then passed through a NAP-5 size exclusion column equilibrated with  $\text{D}_2\text{O}$  for NMR.

**SPAAC Reaction with Azide-Silk:** A stock solution was first prepared by dissolving DBCO-PEG<sub>4</sub>-alcohol (BroadPharm #BP-22800) (25 mg, 50  $\mu\text{mol}$ ) in 100  $\mu\text{L}$  DMSO to make a 0.5 M solution. Small scale reactions containing sub-stoichiometric or excess DBCO were monitored over time with UV to follow the reaction progress. For example, a 0.1  $\mu\text{L}$  aliquot of the DBCO stock solution ( $5 \times 10^{-5}$  mmol;  $\approx 0.04$  eq relative to tyr) was combined with 99.9  $\mu\text{L}$  azide-silk in PBS ( $\approx 2\%$  w/v;  $\approx 5.1 \times 10^{-6}$  mmol silk;  $1.4 \times 10^{-3}$  mmol tyr), and a 5  $\mu\text{L}$  aliquot of the DBCO stock solution ( $2.5 \times 10^{-3}$  mmol;  $\approx 1.7$  eq relative to tyrosine) was combined with 95  $\mu\text{L}$  azide-silk in PBS ( $\approx 2\%$  w/v; est.  $5.1 \times 10^{-6}$  mmol silk and  $1.4 \times 10^{-3}$  mmol tyr). After mixing, 5  $\mu\text{L}$  of the reaction solutions were diluted with 95  $\mu\text{L}$  of PBS and placed in a 96-well plate. The UV absorbance spectra (230–500 nm) of the reaction mixtures at room temperature were acquired over a 24 h period with a plate reader. For larger scale reactions, 50  $\mu\text{L}$  of the DBCO stock solution in DMSO ( $2.5 \times 10^{-2}$  mmol DBCO,  $\approx 1.7$  eq relative to tyr) was added to 950  $\mu\text{L}$  azide-silk in PBS ( $\approx 2\%$  w/v; est.  $4.9 \times 10^{-5}$  mmol silk,  $1.3 \times 10^{-2}$  mmol tyrosine). The mixture was allowed to react between 90 min and 4 h at rt, vortexing periodically. The product was purified using a NAP-10 column (Cytiva) equilibrated with PBS. An aliquot (0.5 mL) was passed through a NAP-5 size exclusion column equilibrated with  $\text{D}_2\text{O}$  for NMR.

**Preparation and Modification of Electrospun Silk Mats:** Over a 20 min period with stirring, 1 mL of 5% w/v poly(ethylene) oxide (PEO, MW 900k) solution in water was slowly dissolved in 4 mL of a 8%–9% w/v silk solution. The solution was then transferred to a syringe and spun into aligned fiber mats using a Spraybase electrospinning instrument with an 18 gauge stainless steel emitter needle located 20 cm from the barrel, a flow rate of 12  $\mu\text{L min}^{-1}$ , applied voltage of 18.0 kV, and spinning the collection barrel at 3000 rpm. The humidity in the chamber during spinning was maintained at 30% using dry nitrogen gas. Once electrospinning was finished, the thin aligned silk mat was carefully peeled from the barrel and stored in a large Petri dish. Small squares ( $\approx 3 \times 3$  cm) were cut from the mat, soaked in 90% methanol for 10 min to crystallize the silk and render the fibers insoluble in water, and then rinsed with DI water 3 $\times$ . The mats were then soaked in DI water inside of a  $37^\circ\text{C}$  thermal rocker for  $\approx 2$  d with light rocking to extract the PEO used during the spinning process. The water inside of the Petri dish was changed after the first day.

To carry out the diazonium coupling reaction on the fiber surfaces, the mats were rinsed with DI water 3 $\times$  and placed in a separate Petri dish containing 8 mL of  $100 \times 10^{-3}$  M borate buffer (pH 9.5). The reaction vessel was placed on ice. The diazonium salt solution was prepared as described in the Diazonium Coupling Reaction section above, but with all amounts of reagents and buffer divided by two. The diazonium salt solution (2 mL total volume) was poured into the Petri dish containing the silk mat submerged in borate buffer and the solution was swirled gently for mixing. The silk mat was left to react for 40 min. Afterward, the reaction solution was decanted, and the silk mat was rinsed thoroughly with DI water 3 $\times$ . For short-term storage, the acid-modified silk mat was kept in DI water. For long-term storage, the mat was dried.

The newly formed azo bonds on the silk were then reduced to amine functional groups. The azo-silk mat was first soaked in BBS (pH 9) for 15 min. In a separate centrifuge tube, 254 mg (1.46 mmol) of sodium hydrosulfite was dissolved in 6 mL BBS. The borate buffer was removed from the Petri dish containing the azo-silk mat and was replaced by the buffered sodium dithionite solution. The silk mat was left to react for 30 min. The reaction solution was then pipetted out of the dish and the silk mat was rinsed 3x with borate buffer.

Further amidation reactions could be carried out using any desired NHS-ester reagent. A 3 × 3 cm mat was first soaked in 2 mL PBS for 30 min at rt. The buffer was decanted and the desired NHS-ester [ex. 20 mg (35 μmol) azido-dPEG 8-NHS ester] was pre-dissolved in 2 mL PBS, and the solution was added to the mat, and left to react for 3 h. The reaction solution was removed and the modified mat was gently rinsed with water 3x.

**Preparation and Modification of Silk Microparticles:** A 1:1 volume ratio of a 8%–9% w/v aqueous silk solution and a 50% w/v aqueous solution of PEG (MW 12k) were combined in a 15 mL centrifuge tube (2 mL of each), vortexed for 30 s, and then sonicated in a water bath for 1 min. The turbid solution was allowed to sit overnight at rt, resuspending periodically. The next day, the solution was centrifuged (10 min at 4000 rpm) and the PEG/water supernatant was removed with pipette. The particles were resuspended in 5 mL water, centrifuged, and the supernatant was removed. This washing procedure was repeated 5x or until the washes were no longer hazy. The resulting particles were then suspended in water, lyophilized and imaged with SEM.

To modify the particles with the diazonium salt, 10 mg of dry microparticles were suspended in 800 μL of BBS (pH 9), and then placed on ice. The diazonium salt was prepared as described in the Diazonium Coupling Reaction section, but the amount of all reagents was divided by 20 giving a total volume of 200 μL. This diazonium salt solution was added to the silk microparticles in BBS and left to react for 40 min on ice. To purify the particles, the reaction mixture was centrifuged for 1 min in a mini centrifuge, and the supernatant was removed. Particles were washed by resuspending vigorously in 1 mL water, followed by another round of centrifugation and removal of the supernatant. This wash was repeated at least 3x.

The washed azo-silk particles were then suspended in 1000 μL BBS (pH 9) to prepare for the next reduction reaction. To the ≈10 mg of azo-silk microparticles suspended in BBS, 20 mg (115 μmol) of sodium hydrosulfite was added and the mixture was vortexed. The reaction was left for 1 h at rt, vortexing periodically. The reaction mixture was then centrifuged for 1 min in a mini centrifuge, the supernatant was removed. The particles were resuspended in water, centrifuged, and the supernatant was removed. This washing procedure was repeated at least 3x.

The washed Am-Tyr silk particles were then suspended in 1000 μL PBS (pH 7.2) to carry out the final amidation reaction. To the ≈10 mg of AmTyr-modified silk microparticles in PBS was added 11 mg (19.5 μmol) azido-dPEG8-NHS ester. This particular reagent is used as an example but could be swapped for any other NHS-ester desired. The mixture was vortexed to dissolve, and then left to react for 3 h at rt, vortexing periodically. The final particles were washed with water as described previously and lyophilized for storage.

To characterize each modification step, direct UV measurements were carried out on the solid particles suspended in PBS in a 96-well plate using a plate reader, but the peaks were broad and ill-defined due to the opacity of the particles. To obtain better spectra, the microparticles were dissolved by adding 0.5 mL of 9.3 M LiBr to dry particles (≈0.5 mg) followed by vortexing. If not dissolved after ≈20 min, samples were heated at 60 °C for ≈1 h. The resulting solution of the modified silk dissolved in LiBr (50 μL) was combined with 50 μL PBS in a well plate, and the UV spectrum was recorded using a plate reader.

## Supporting Information

Supporting Information is available from the Wiley Online Library or from the author.

## Acknowledgements

This work was supported by the National Science Foundation under Grant No. DMR-1807878. The authors are grateful for assistance from John Antos, Hla Win-Piazza, and Sam Danforth with analytical techniques and instrumentation. The NMR data acquisition on the 500 MHz NMR spectrometer was made possible through an NSF-MRI award (Award No. 1532269). The authors also thank Mike Kraft in Scientific Technical Services at WWU for assistance with SEM. The authors also acknowledge the use of facilities in Washington State that are part of the Joint Center for Deployment and Research in Earth Abundant Materials (JCDREAM).

## Conflict of Interest

The authors declare no conflict of interest.

## Data Availability Statement

The data that support the findings of this study are available from the corresponding author upon reasonable request.

## Keywords

amino-tyrosine, azobenzene, HMBC, NHS-ester, silk, tyrosine

Received: April 8, 2022

Revised: May 13, 2022

Published online:

- [1] G. H. Altman, F. Diaz, C. Jakuba, T. Calabro, R. L. Horan, J. Chen, H. Lu, J. Richmond, D. L. Kaplan, *Biomaterials* **2003**, *24*, 401.
- [2] Y. Wang, H.-J. Kim, G. Vunjak-Novakovic, D. L. Kaplan, *Biomaterials* **2006**, *27*, 6064.
- [3] R. D. Abbott, E. P. Kimmerling, D. M. Cairns, D. L. Kaplan, *ACS Appl. Mater. Interfaces* **2016**, *8*, 21861.
- [4] X. Zhang, M. R. Reagan, D. L. Kaplan, *Adv. Drug Delivery Rev.* **2009**, *61*, 988.
- [5] T. Yucel, M. L. Lovett, D. L. Kaplan, *J. Controlled Release* **2014**, *190*, 381.
- [6] E. Wenk, H. P. Merkle, L. Meinel, *J. Controlled Release* **2011**, *150*, 128.
- [7] B. Zhu, H. Wang, W. R. Leow, Y. Cai, X. J. Loh, M.-Y. Han, X. Chen, *Adv. Mater.* **2015**, *28*, 4250.
- [8] C.-Z. Zhou, F. Confalonieri, M. Jacquet, R. Perasso, Z.-G. Li, J. Janin, *Proteins* **2001**, *44*, 119.
- [9] A. R. Murphy, D. L. Kaplan, *J. Mater. Chem.* **2009**, *19*, 6443.
- [10] M. A. Serban, D. L. Kaplan, *Biomacromolecules* **2010**, *11*, 3406.
- [11] D. L. Heichel, K. A. Burke, *Bioconjugate Chem.* **2020**, *31*, 1307.
- [12] Y. H. Youn, S. Pradhan, L. P. Da Silva, I. K. Kwon, S. C. Kundu, R. L. Reis, V. K. Yadavalli, V. M. Correlo, *ACS Biomater. Sci. Eng.* **2021**, *7*, 2466.
- [13] C. J. Love, B. A. Serban, T. Katashima, K. Numata, M. A. Serban, *ACS Biomater. Sci. Eng.* **2019**, *5*, 5960.
- [14] K. Zheng, Y. Chen, W. Huang, Y. Lin, D. L. Kaplan, Y. Fan, *ACS Appl. Mater. Interfaces* **2016**, *8*, 14406.
- [15] S. Sofia, M. B. McCarthy, G. Gronowicz, D. L. Kaplan, *J. Biomed. Mater. Res.* **2001**, *54*, 139.
- [16] L. Meinel, V. Karageorgiou, S. Hofmann, R. Fajardo, B. Snyder, C. Li, L. Zichner, R. Langer, G. Vunjak-Novakovic, D. L. Kaplan, *J. Biomed. Mater. Res.* **2004**, *71A*, 25.
- [17] X. Wang, D. L. Kaplan, *Macromol. Biosci.* **2010**, *11*, 100.

- [18] B. Subia, S. Chandra, S. Talukdar, S. C. Kundu, *Integr. Biol.* **2014**, *6*, 203.
- [19] K. A. Burke, D. C. Roberts, D. L. Kaplan, *Biomacromolecules* **2016**, *17*, 237.
- [20] S. Santi, I. Mancini, S. Dirè, E. Callone, G. Speranza, N. Pugno, C. Migliaresi, A. Motta, *ACS Biomater. Sci. Eng.* **2021**, *7*, 507.
- [21] T. Martínez Martínez, Á. García Aliaga, I. López-González, A. A. Tarazona, M. J. Ibáñez Ibáñez, J. L. Cenis, L. Meseguer-Olmo, A. A. Lozano-Pérez, *ACS Biomater. Sci. Eng.* **2020**, *6*, 3299.
- [22] H. Zhao, E. Heusler, G. Jones, L. Li, V. Werner, O. Germershaus, J. Ritzer, T. Luehmann, L. Meinel, *J. Struct. Biol.* **2014**, *186*, 420.
- [23] C. Vepari, D. Matheson, L. Drummy, R. Naik, D. L. Kaplan, *J. Biomed. Mater. Res.* **2010**, *93A*, 595.
- [24] T. Wongpinyochit, P. Uhlmann, A. J. Urquhart, F. P. Seib, *Biomacromolecules* **2015**, *16*, 3712.
- [25] Y. Gotoh, Y. Ishizuka, T. Matsuura, S. Niimi, *Biomacromolecules* **2011**, *12*, 1532.
- [26] H. Sogawa, N. Ifuku, K. Numata, *ACS Biomater. Sci. Eng.* **2019**, *5*, 5644.
- [27] D. L. Heichel, K. A. Burke, *ACS Biomater. Sci. Eng.* **2019**, *5*, 3246.
- [28] B. P. Partlow, C. W. Hanna, J. Rnjak-Kovacina, J. E. Moreau, M. B. Applegate, K. A. Burke, B. Marelli, A. N. Mitropoulos, F. G. Omenetto, D. L. Kaplan, *Adv. Funct. Mater.* **2014**, *24*, 4615.
- [29] P. Wang, C. Deng, J. Yuan, Y. Yu, L. Cui, M. Su, Q. Wang, X. Fan, *Biotechnol. Appl. Biochem.* **2015**, *63*, 163.
- [30] A. R. Murphy, P. St John, D. L. Kaplan, *Biomaterials* **2008**, *29*, 2829.
- [31] K. Tsioris, G. E. Tilburey, A. R. Murphy, P. Domachuk, D. L. Kaplan, F. G. Omenetto, *Adv. Funct. Mater.* **2010**, *20*, 1083.
- [32] E. Wenk, A. R. Murphy, D. L. Kaplan, L. Meinel, H. P. Merkle, L. Uebbersax, *Biomaterials* **2010**, *31*, 1403.
- [33] S. Sampaio, T. M. R. Miranda, J. G. Santos, G. M. B. Soares, *Polym. Int.* **2011**, *60*, 1737.
- [34] I. S. Romero, M. L. Schurr, J. V. Lally, M. Z. Kotlik, A. R. Murphy, *ACS Appl. Mater. Interfaces* **2013**, *5*, 553.
- [35] P. N. Atterberry, T. J. Roark, S. Y. Severt, M. L. Schiller, J. M. Antos, A. R. Murphy, *Biomacromolecules* **2015**, *16*, 1582.
- [36] J. M. Coburn, E. Na, D. L. Kaplan, *J. Controlled Release* **2015**, *220*, 229.
- [37] A. R. D. Reeves, K. L. Spiller, D. O. Freytes, G. Vunjak-Novakovic, D. L. Kaplan, *Biomaterials* **2015**, *73*, 272.
- [38] W. Chen, Z. Wang, Z. Cui, D. Pan, K. Millington, *Polym. Degrad. Stab.* **2015**, *121*, 187.
- [39] J. E. Brown, J. E. Moreau, A. M. Berman, H. J. Mcsherry, J. M. Coburn, D. F. Schmidt, D. L. Kaplan, *Adv. Healthcare Mater.* **2017**, *6*, 1600762.
- [40] M. J. Landry, M. B. Applegate, O. S. Bushuyev, F. G. Omenetto, D. L. Kaplan, M. Cronin-Golomb, C. J. Barrett, *Soft Matter* **2017**, *13*, 2903.
- [41] G. Palermo, L. Barberi, G. Perotto, R. Caputo, L. De Sio, C. Umeton, F. G. Omenetto, *ACS Appl. Mater. Interfaces* **2017**, *9*, 30951.
- [42] E. D. Patamia, N. A. Ostrovsky-Snider, A. R. Murphy, *ACS Appl. Mater. Interfaces* **2019**, *11*, 33612.
- [43] J. M. Hooker, E. W. Kovacs, M. B. Francis, *J. Am. Chem. Soc.* **2004**, *126*, 3718.
- [44] C. R. Behrens, J. M. Hooker, A. C. Obermeyer, D. W. Romanini, E. M. Katz, M. B. Francis, *J. Am. Chem. Soc.* **2011**, *133*, 16398.
- [45] R. A. S. Robinson, A. R. Evans, *Anal. Chem.* **2012**, *84*, 4677.
- [46] N. Abello, B. Barroso, H. A. M. Kerstjens, D. S. Postma, R. Bischoff, *Talanta* **2010**, *80*, 1503.
- [47] L. Haandel, J. Killmer, X. Li, C. Schöneich, J. F. Stobaugh, *Chroma* **2008**, *68*, 507.
- [48] A. Yamaguchi, T. Matsuda, K. Ohtake, T. Yanagisawa, S. Yokoyama, Y. Fujiwara, T. Watanabe, T. Hohsaka, K. Sakamoto, *Bioconjugate Chem.* **2016**, *27*, 198.
- [49] Y. Liu, P. Zhou, H. Da, H. Jia, F. Bai, G. Hu, B. Zhang, J. Fang, *Chem. - Eur. J.* **2019**, *118*, 1338.
- [50] A. C. Obermeyer, J. B. Jarman, M. B. Francis, *J. Am. Chem. Soc.* **2014**, *136*, 9572.
- [51] L. S. Wray, X. Hu, J. Gallego, I. Georgakoudi, F. G. Omenetto, D. Schmidt, D. L. Kaplan, *J. Biomed. Mater. Res., Part B* **2011**, *99*, 89.
- [52] G. J. Pielak, M. S. Urdea, J. I. Legg, *Biochemistry* **2002**, *23*, 596.
- [53] V. Hong, S. I. Presolski, C. Ma, M. G. Finn, *Angew. Chem.* **2009**, *121*, 10063.
- [54] K. Yamagishi, K. Sawaki, A. Murata, S. Takeoka, *Chem. Commun.* **2015**, *51*, 7879.
- [55] H. Zhang, S. Neal, D. S. Wishart, *J. Biomol. NMR* **2003**, *25*, 173.
- [56] E. F. Mooney, P. H. Winson, *Annu. Rep. NMR Spectrosc.* **1969**, *2*, 125.
- [57] X. Hu, D. Kaplan, P. Cebe, *Macromolecules* **2006**, *39*, 6161.
- [58] J. Wu, Z. Zheng, G. Li, D. L. Kaplan, X. Wang, *Acta Biomater.* **2016**, *39*, 156.
- [59] S. Y. Severt, S. L. Maxwell, J. S. Bontrager, J. M. Leger, A. R. Murphy, *J. Mater. Chem. B* **2017**, *5*, 8105.